JTTEE5 15:501-506
DOI: 10.1361/105996306X147298
1059-9630/$19.00 © ASM International

Kinetic Sprayed Rare Earth Iron Alloy Composite Coatings

T. Van Steenkiste

(Submitted February 22, 2006; in revised form April 18, 2006

One unique advantage of the kinetic spray process is its ability to mix constituents that would normally react with each other to form coatings. This attribute was used to produce composite coatings with different rare earth iron alloys ($REFe_2$) and several ductile matrices. Composite coatings of Terfenol-D [$(Tb_{0.3}Dy_{0.7})Fe_{1.9}$] and $SmFe_2$ were combined with ductile matrices of aluminum, copper, iron, and molybdenum. Evidence of an induced magnetic coercivity was measured for the $REFe_2$-Mo and Fe composite coatings. Coatings were produced on flat substrates and shafts. Coating morphology as well as the physical, magnetostrictive, and magnetic properties of these coatings are discussed.

Keywords cold gas dynamic spraying, composite materials, influence of spray parameters

1. Introduction

The kinetic spray process (Ref 1-3) utilizes high-pressure gas to accelerate powder particles to velocities of ~500 m/s and is being used to produce low-porosity, low-oxide, and low residual stress coatings. The cold spray process, or CGSM (Ref 4-7), is a related process, and both have been discussed in detail in the literature (Ref 1-7). The initial powders are not melted or generally thermally softened in these processes. Any original phase or phases present in the starting powder is preserved in the coatings. Another advantage of the kinetic spray process is the ability to mix materials that would normally react with each other and form a composite coating. Each constituent of the composite coating retains the original material properties it had prior to formation of the coating because no melting is involved in the coating process.

The kinetic spray process allows production of composite coatings using a combination of rare earth iron alloys such as Terfenol-D [$(Tb_{0.3}Dy_{0.7})Fe_{1.9}$] and $SmFe_2$ and a ductile matrix (aluminum, copper, etc.). Such a coating would combine the "giant" saturation magnetostriction, the magnetic and physical properties of rare earth iron alloys, and the strength and ductile properties of the matrices (aluminum, copper, etc.). A coating using the brittle rare earth iron alloys would be strengthened when incorporated into the ductile metal matrix. Such coatings, with the appropriate detector, could function as torque, position, or force sensors when incorporated into the ductile metal matrix.

This article was originally published in *Building on 100 Years of Success: Proceedings of the 2006 International Thermal Spray Conference* (Seattle, WA), May 15-18, 2006, B.R. Marple, M.M. Hyland, Y.-Ch. Lau, R.S. Lima, and J. Voyer, Ed., ASM International, Materials Park, OH, 2006.

T. Van Steenkiste, Delphi Research Labs, Shelby Township, MI. Contact e-mail: thomas.van.steekiste@delphi.com.

2. Experimental Methods

Figure 1 is a photograph of the kinetic spraying of a Terfenol-D/aluminum coating onto a nitronic (nonmagnetic austenitic stainless steel alloy) shaft. The pyrophoric nature of the Terfenol-D is clearly visible as the coating is applied to the shaft. The kinetic spray nozzle used for all the coatings produced in this study was 301 mm long with an exit area of 12.7 × 5 mm. The throat diameter was 2 mm. The $SmFe_2$ powders were made in house by melting, annealing, and ball milling the ingot into powder and sieving into a size range from ~63 to 90 μm. The Terfenol-D ingot powder particles (received from Etrema Inc., Ames, IA) were between ~65 and 300 μm in diameter and combined with a range of ductile materials. The ductile materials ranged in size between ~63 and 90 μm and were received from the FJ Brodmann Company (Harvey, LA). Stand-off distance was ~25 mm. Traverse speed varied from 0.5 to 6 mm/s. The main gas in all cases was helium, and the powder feeder gas was nitrogen.

All the rare earth alloys and the ductile materials were mixed in a 50/50 (by volume) ratio prior to spraying. Terfenol-D coatings were produced with ductile matrices of copper, aluminum, nickel, tantalum, molybdenum, and iron. $SmFe_2$ composite coat-

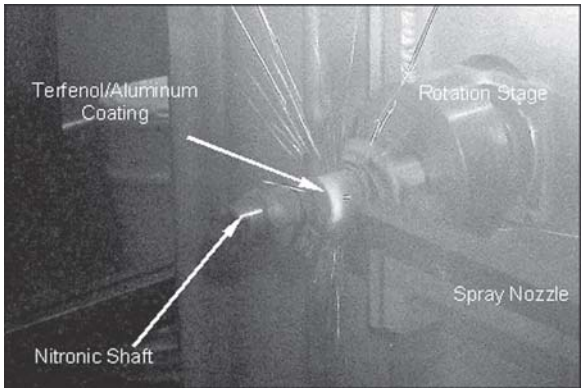

Fig. 1 Kinetic spraying of Terfenol-D/aluminum coating on nitronic shaft

ings were only investigated with the copper matrix. The powder feed rate was set at 500 rpm on the auger screw for all coatings (~1.5 g/s). The main gas temperature ranged between 204 and 593 °C depending on the material combination being sprayed. The number of passes varied from 2 to as high as 20. Shafts were sandblasted in the coated area, clamped into a rotary vise, rotated at 300 rpm, and sprayed. The flat brass substrates were sandblasted prior to spraying. Porosity and density measurements were made using an AccuPyc 1330 helium pycnometer (Micromeritics, Norcross, GA) for the copper and aluminum composites.

Thick samples of the coatings were removed from the brass substrates by bending the substrate to induce a crack to form along the coating/substrate interface until the coating delaminated. The coatings were then subsequently sectioned into plates for testing of their magnetostriction properties. Strain gauges (in half-bridge configuration) were attached to the samples (oriented 90° relative to each other), and the coatings were placed in a uniform magnetic field, H. $\lambda_{\parallel}$ is the strain parallel to the H direction of the magnetic field, and $\lambda_{\perp}$ is the strain perpendicular to the H direction of the magnetic field. For an isotropic magnetostrictive coating in a magnetic field large enough to saturate the material, the difference $(\lambda_{\parallel} - \lambda_{\perp})$ is proportional to the saturation magnetostriction λ_S, where $\lambda_S = 2/3(\lambda_{\parallel} - \lambda_{\perp})$ (Ref 9).

3. Results and Discussion

Figure 2(a) is a SEM micrograph of the cross section of a Terfenol-D/aluminum composite coating on a brass substrate. The darker areas in the SEM photo are the aluminum matrix, and lighter areas are the Terfenol-D. Figure 2(b) and (c) are energy-dispersive spectroscopy x-ray mapping (EDAX) photos for dysprosium and aluminum, respectively. One can clearly identify the Terfenol-D particles (dysprosium map) in Fig. 2(b) and the aluminum particles in Fig. 2(c). Porosity for this sample was measured to be 0.6% with the final coating composition consisting of ~27% Terfenol-D and 72% aluminum (vol.%); recall that the original starting mixture was 50% Terfenol-D and 50% aluminum (vol.%). Some cracking is observed in the Terfenol-D due to its brittle behavior; however, some cracking may be an artifact of the sectioning or polishing of the sample (i.e., pull-outs). The Terfenol-D was uniformly dispersed throughout the aluminum matrix.

Figure 3 is a graph of the strain $2/3(\lambda_{\parallel} - \lambda_{\perp})$ (ppm) plotted against magnetic field strength (kOe). The series of curves plotted in Fig. 3 are for Terfenol-D/aluminum composite coatings produced as a function of increasing main gas (helium) temperatures. The sample curves are similar, and one observes that increasing the main gas temperature (i.e., particle velocity) usually results in little effect on the magnetostriction response. Also shown in Fig. 3 (dotted line) is the strain response of T-250 maraging steel for comparison. The curves show a lack of coercivity in these coatings. In a material with a high degree of coercivity, a hysteresis (butterfly-shaped loop) would be observed on each side of the vertical axis. This lack of coercivity was also observed in the ingot powder, which shows equally small coercivity.

The Terfenol-D/aluminum coating's thickness, density, and porosity measurements are shown in Table 1 as a function of the main gas temperature. Porosity measurements for the coatings were approximately the same within the accuracy of the measurement (±0.3%).

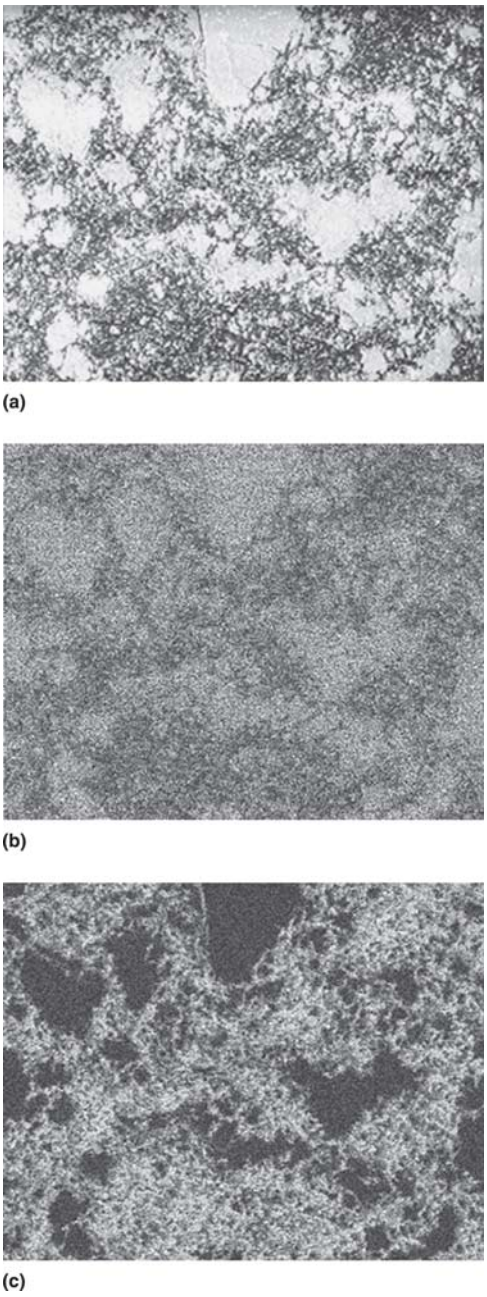

Fig. 2 (a) SEM micrograph of a Terfenol-D/aluminum composite coating; (b) light areas are Terfenol-D (dysprosium map); (c) the lighter areas are aluminum (aluminum map).

Figure 4(a) is a micrograph of a Terfenol-D/copper composite coating. A microstructure similar to that in the Terfenol-D/aluminum coating is observed. The lighter regions are copper, and the darker regions are Terfenol-D material. The Terfenol-D/copper coating's density and porosity measurement values are shown in Table 2. These coatings were sprayed at a main gas temperature of 315 °C. Porosity of the coatings was approximately twice that of the Terfenol-D/aluminum coatings; how-

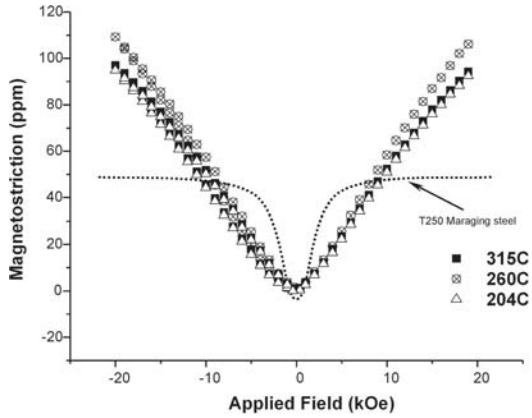

Fig. 3 Magnetostriction data as a function of spraying conditions for Terfenol-D/aluminum composite coatings (dotted line is the typical magnetostriction data for T-250 maraging steel for comparison)

Table 1 Terfenol-D/aluminum composite coating properties

Gas temp, °C	Thickness, µm	Density, g/cm^3	Porosity, %	Al, %	Terfenol-D, %
315	1770	4.57	0.98	70	30
260	1675	4.54	0.98	70	30
204	1780	4.44	1.14	72	26

ever, the percentage of Terfenol-D incorporated into the coatings was noticeably higher, 37.3% average (copper) compared with 28.3% average (aluminum). This increased incorporation of Terfenol-D into the copper matrix may be a result of the physical properties of the matrix. Comparing the Young's modulus of copper (131.3 GPa) to that of aluminum (72.2 GPa; Ref 8) shows that the copper matrix is a factor ~1.8 times stronger. The matrix must be able to absorb the kinetic energy of the Terfenol-D particles to be incorporated into the coating because the Terfenol-D does not plastically deform. Perhaps this is why the percentage of Terfenol-D incorporated is higher for the copper matrix than the aluminum matrix. The strain (Fig. 4b) is approximately half that of the Terfenol-D/aluminum coatings with no significant coercivity demonstrated as noted from the symmetric response around $H = 0$.

Composite coatings of $SmFe_2$/copper were also produced using an original starting mixture of 50% $SmFe_2$ and 50% copper (by volume). Figure 5(a) is a micrograph of the coating cross section. The dark regions are samarium iron, and the lighter regions are copper. Figure 5(b) is the magnetostrictive strain as a function of the applied magnetic field. The strain is approximately the same in magnitude as the other Terfenol-D/copper composite, however opposite in sign due to the negative magnetostriction coefficient of the samarium iron. The material has not saturated at 15 kOe, an effect similar to that observed with hot pressed composites (Ref 9-11). Coercivity is not observed in this sample as evidenced by the lack of any deviation in the butterfly-shaped curves around $H = 0$.

Figure 6(a) is a micrograph of a Terfenol-D/iron composite. The morphology of the coating is similar to the composite coatings produced using aluminum and copper matrices. The dark

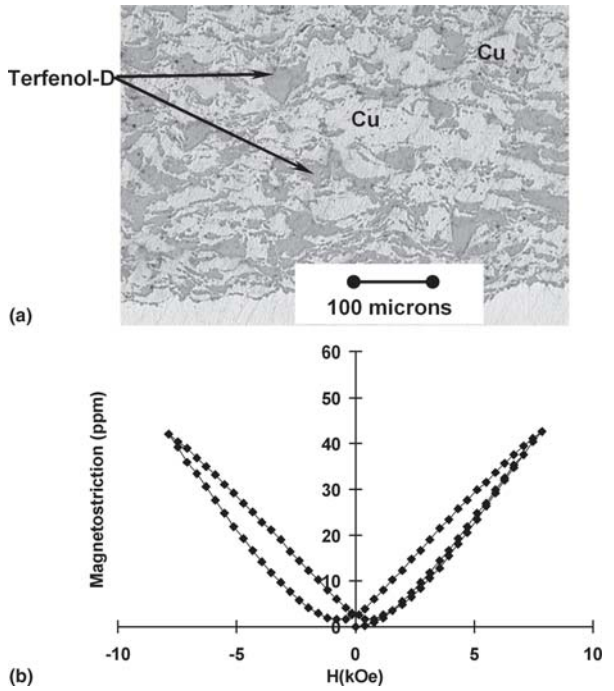

Fig. 4 (a) SEM micrograph of a Terfenol-D/copper composite coating (darker areas are the Terfenol-D, and lighter areas are copper); (b) magnetostriction response of a Terfenol-D/copper composite coating as a function of the applied magnetic field

Table 2 Terfenol-D/copper composite coating properties

Density, g/cm^3	Porosity, vol.%	Copper, vol.%	Terfenol-D, vol.%
8.83	2.52	62.7	37.3
8.82	1.99	63.7	36.3
8.83	2.79	61.7	38.3

regions are the Terfenol-D, and the lighter regions are iron. The magnetostrictive strain is plotted in Fig. 6(b) as a function of the applied field. The shape and amplitude of the curve are similar to those of the copper composite; however, a small coercivity is measured, <1 kOe. As the magnetic field is decreased, the magnetostriction also decreases; however, it is observed that a small reverse magnetic field is needed to completely drive magnetostriction to zero. The effect is also measured when the field is ramped from the negative magnetic field direction to positive field direction, where a slight positive field is required to drive the magnetostriction to zero. Presumably, this is caused by the iron/Terfenol-D interaction (Terfenol-D ingot has a slight coercivity, see Fig. 9a) in the coating sample. The butterfly shape of the curves around $H = 0$ is characteristic of rare earth composites/iron that have coercivity and have been produced by hot pressing (Ref 9-11). Figure 7(b) and (c) shows EDAX mapping for dysprosium and iron, respectively. One can clearly identify the iron particles by comparing Fig. 7(b) (iron mapping) and the Terfenol-D particles (dysprosium mapping) in Fig. 7(c) with the SEM micrograph in Fig. 7(a).

Figure 8(a) is an optical micrograph of the Terfenol-D/molybdenum composite coating. The dark regions in the micrograph are Terfenol-D, and the lighter regions are the molybde-

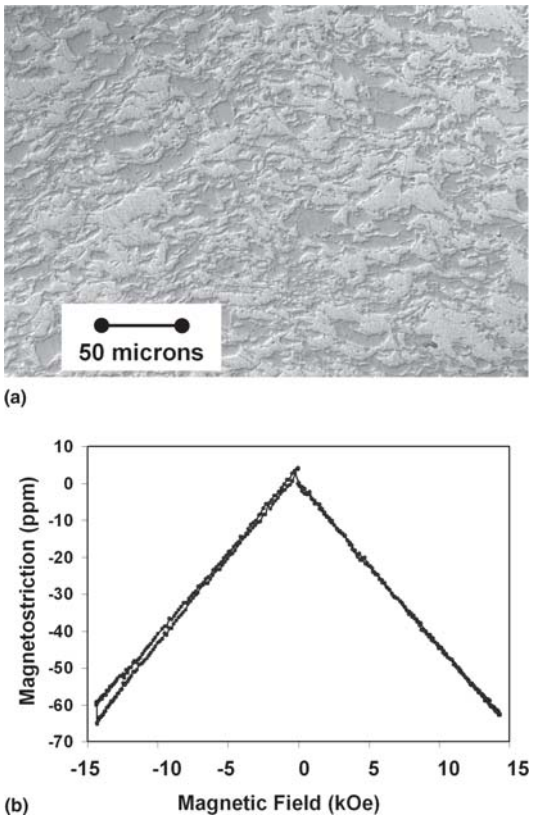

Fig. 5 (a) Micrograph of a $SmFe_2$/copper composite coating (darker areas are samarium, and lighter areas are copper); (b) magnetostriction response of a $SmFe_2$/copper composite coating as a function of the applied magnetic field

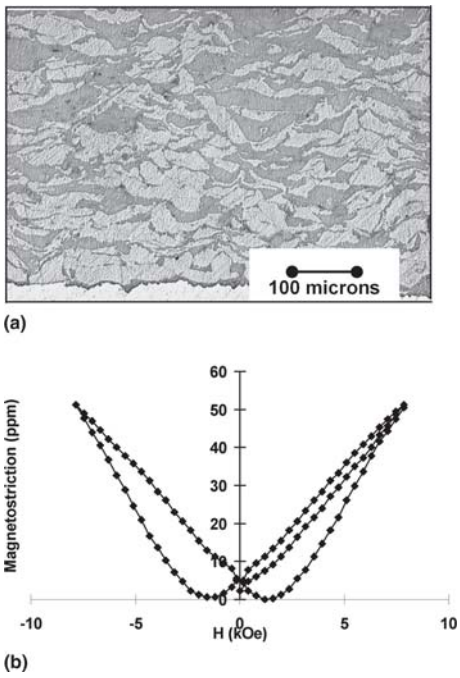

Fig. 6 (a) SEM micrograph of a Terfenol-D/iron composite coating (darker areas are Terfenol-D, and lighter areas are iron); (b) magnetostriction response of a Terfenol-D/iron composite coating as a function of the applied magnetic field

num particles. The magnetostrictive response as a function of the applied magnetic field is shown in Fig. 8(b). The magnetostrictive behavior of the Terfenol-D/molybdenum curves demonstrates a large coercivity effect as evidenced by the relatively large reverse magnetic field needed to reduce the magnetostriction to a minimum as the field reverses from +8 to −8 kOe. The effect is also observed as the magnetic field goes from −8 to + 8 kOe. Here, a relative large positive field is required to reduce the magnetostriction to a minimum. The magnitude of the Terfenol-D/molybdenum coating is significantly larger than the Terfenol-D/iron coating. It is interesting to note that of all the coatings tested only the Terfenol-D/molybdenum, and the Terfenol-D/iron composites demonstrated a significant coercivity after being kinetically sprayed.

In an effort to determine the origin of the kinetically sprayed coercivity, a vibrating sample magnetometer was used to measure the demagnetization curves of the Terfenol-D ingot powder, Terfenol-D powder mixed with the molybdenum powder, and a sample piece of the Terfenol-D/molybdenum composite coating. The results are shown in Fig. 9. In this figure, curve b is a nickel powder for comparison. The vibrating sample magnetometer measures the magnetic moment as a function of applied field. No significant coercivity is measured for the Terfenol-D ingot powder (curve a) or the Terfenol-D powder mixed with the molybdenum powder (curve c). Only after kinetically spraying the powders does the composite coating demonstrate a coercivity of H_{ci} = 3.7 kOe (curve d).

The Terfenol-D/molybdenum composite coating shown in Fig. 8(a) has a microstructure consisting of Terfenol-D particles surrounded by a matrix of plastically deformed molybdenum particles. The magnetostrictive response to the applied field (Fig. 8b) is significantly different from that of the other composite coatings measured. A relatively large coercivity response is measured in the Terfenol-D/molybdenum composite coating as shown in Fig. 8(b) (note the large hysteresis loop, i.e., the butterfly shape of the curves around H = 0). Indeed, the sample coatings possessed sufficient coercivity that individual pieces of coating would stick together once magnetized. A coercivity of H_{ci} = 3.7 kOe was measured for the coating as shown in Fig. 9. For comparison, the typical value of coercivity for Alnico magnets is ~1 kOe.

Bulk molybdenum is known to be paramagnetic. Molybdenum compounds have been reported to have ferromagnetic behavior (Ref 12, 13). The initial powders do not possess any significant coercivity (Fig. 9c), and it is observed from the coating morphology that the Terfenol-D does not plastically deform although the molybdenum particles do. This raises the question whether the plastic deformation of the molybdenum produces an anisotropic plane in which the magnetic moments of the molybdenum would align. This strain-induced plane perpendicular to the spray direction could provide an easy axis for alignment. Further investigation is planned.

4. Conclusions

The unique advantage of the kinetic spray process is its ability to produce coatings without generally thermally softening or

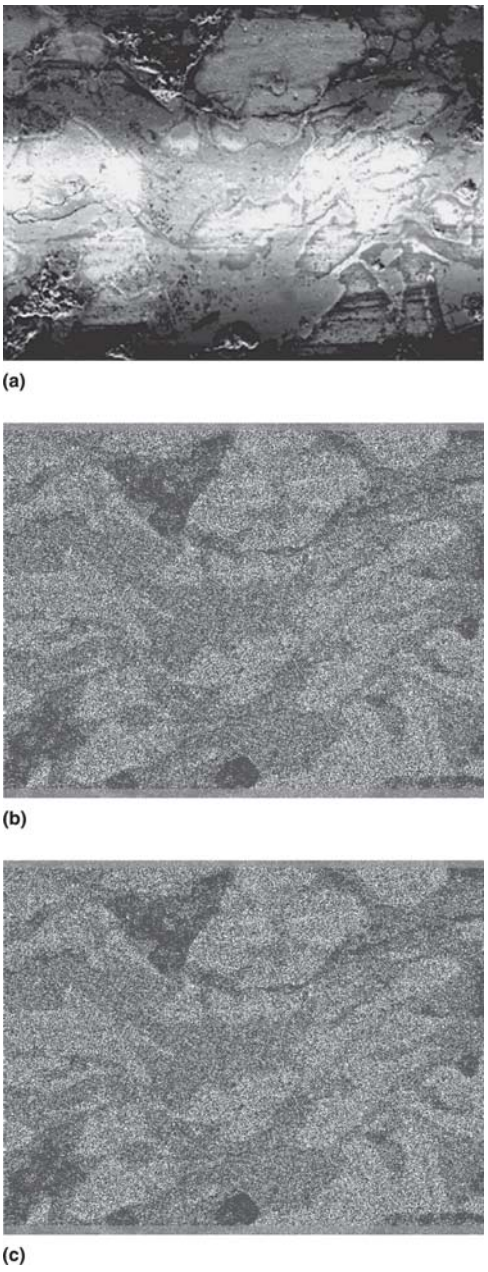

Fig. 7 (a) SEM micrograph of a Terfenol-D/iron composite coating; (b) Fe mapping; (c) dysprosium mapping

melting the original constituents. This advantage was used to produce composite coatings of Terfenol-D ($(Tb_{0.3}Dy_{0.7})Fe_{1.9}$) and $SmFe_2$ with ductile matrices of aluminum, copper, iron, and molybdenum. The constituents did not react with each other and formed robust coatings. The composite coatings produced using the $SmFe_2$ and Terfenol-D powders in matrices of aluminum, copper, iron, and molybdenum demonstrate there is insufficient kinetic energy to plastically deform the brittle rare earth iron alloys (Fig. 2, 4a, 5a, 6a, 7, and 8a). There is, however, sufficient energy to plastically deform the ductile material of the matrices. All of the cross-sectional micrographs of the composite coatings show that the ductile matrix material plastically de-

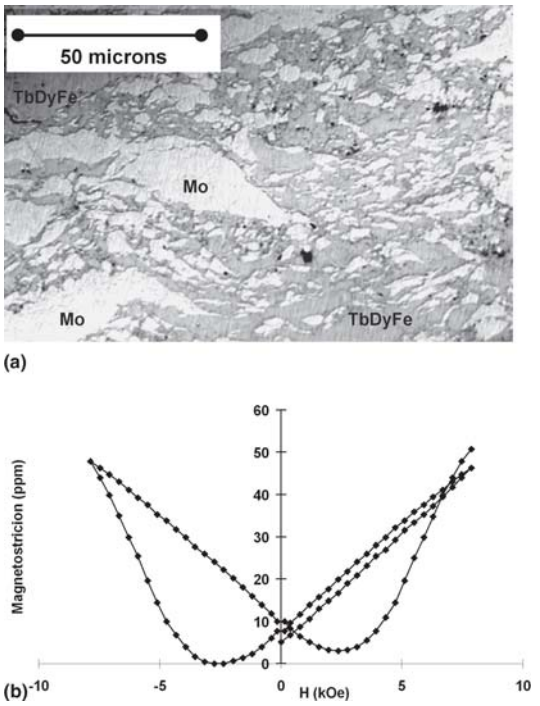

Fig. 8 (a) SEM micrograph of a Terfenol-D/molybdenum composite coating (darker areas are Terfenol-D, and lighter areas are molybdenum); (b) magnetostriction response of a Terfenol-D/molybdenum composite coating as a function of the applied magnetic field

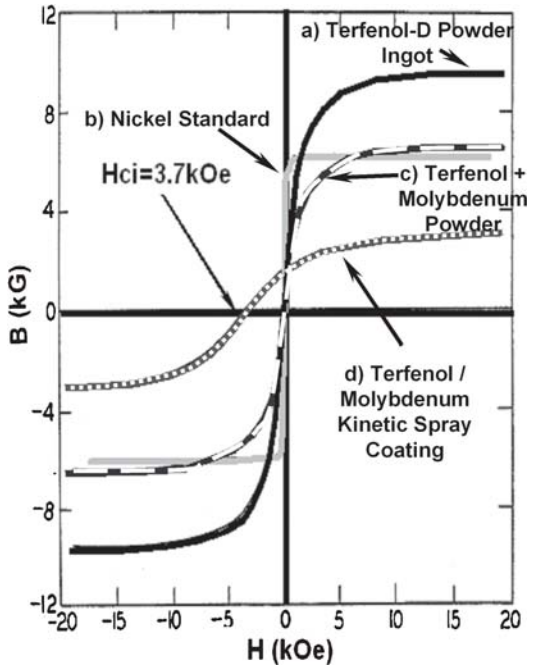

Fig. 9 Demagnetization curves for (a) Terfenol-D ingot powder only, (b) nickel powder standard for comparison, (c) Terfenol-D + molybdenum powder, and (d) Terfenol-D/molybdenum kinetically sprayed coating

forms around the brittle rare earth alloys, resulting in coatings with a low degree of porosity. Some fracturing of the rare earth iron alloys was observed at higher magnifications.

Evidence of an induced magnetic coercivity was measured for the Terfenol-D/Mo and Fe composite coatings. The largest effect was observed with the molybdenum composite. A coercivity value of H_{ci} = 3.7 kOe was measured. Coatings were produced on flat substrates and shafts. The coating morphology and the physical, magnetostrictive, and magnetic properties of these composite coatings were found to be similar.

Because of the pyrophoric nature of the rare earth iron alloys, major modifications will be needed in the dust collector system to handle the kinetic spraying of pyrophoric materials safely. The rare earth alloys are extremely pyrophoric in nature, and suitable safety measures need to be taken to contain the sparks generated upon impact with the substrate. Note the degree of sparking shown in Fig. 1. Adequate baffling is necessary to prevent sparks from reaching the dust collector.

Acknowledgments

This work has significantly benefited from the contributions of Don Morelli and Dan Hogan for magnetic measurements, Fred Pinkerton and Jerome Moleski for some of the early $SmFe_2$ experimental work, and John Smith and Daniel Gorkiewicz for valuable discussions and assistance.

References

1. T.H. Van Steenkiste, J.R. Smith, R.E. Teets, J.J. Moleski, and D.W. Gorkiewicz, Kinetic Spray Coating Method and Apparatus, U.S. Patent 6,139,913, Oct 31, 2000
2. T.H. Van Steenkiste, J.R. Smith, and R.E. Teets, Aluminum Coatings via Kinetic Spray with Relatively Large Powder Particles, *Surf. Coat. Technol.,* 2002, **154,** p 237-252
3. T.H. Van Steenkiste, J.R. Smith, R.E. Teets, J.J. Moleski, D.W. Gorkiewicz, R.P. Tison, D.R. Marantz, K.A. Kowalsky, W.L. Riggs II, P.H. Zajchowski, et al., Kinetic Spray Coatings, *Surf. Coat. Technol.,* 1999, **111,** p 62-71
4. A.P. Alkhimov, V.F. Kosarev, and A.N. Papyrin, A Method of Cold Gas-Dynamic Deposition, *Dokl. Akad. Nauk SSSR,* 1990, **315,** p 1062-1065
5. A.P. Alkhimov, A.N. Papyrin, V.F. Kosarev, N.I. Nesterovich, and M.M. Shushpanov, Gas Dynamic Spraying Method for Applying a Coating, U.S. Patent 5,302,414, Apr 12, 1994
6. R.C. Dykhuizen, M.F. Smith, D.L. Gilmore, R.A. Neiser, X. Jiang, and S. Sampath, Impact of High Velocity Cold Spray Particles, *J. Therm. Spray Technol.,* 1998, **7,** p 559-564
7. H. Kreye and T. Stoltenhoff, Cold Spray-Study of Process and Coating Characteristics, *Thermal Spray: Surface Engineering via Applied Research,* C.C. Berndt, Ed., ASM International, 2000, p 419
8. A. Buch, *Pure Metals Properties: A Scientific and Technical Handbook,* ASM International, 1999
9. F.E. Pinkerton, T.W. Capehart, J.F. Herbst, E.G. Brewer, and C.B. Murphy, Processing Effects on Magnetostrictive and Physical Properties of $SmFe_2$/Metal Composites, *J. Appl. Phys.,* 1998, **83**(11), p 7252-7254
10. F.E. Pinkerton, J.F. Herbst, T.W. Capehart, M.S. Meyer, and W.A. Fellberg, Magnetostrictive $Sm_{1-x}Nd_xFe_2$/Fe Composites from Melt Spun Precursors, *J. Appl. Phys.,* 1999, **85**(3), p 1654-1657
11. F.E. Pinkerton, T.W. Capehart, J.F. Herbst, E.G. Brewer, and C.B. Murphy, Magnetostrictive $SmFe_2$/Metal Composites, *Appl. Phys. Lett.,* 1997, **70**(19), p 2601-2603
12. S.E. Loflans, T. Scabarozi, K.V. Ramanujachary, and W.H. McCarroll, Unusual Magnetic Properties of $La_5Mo_4O_{16}$, *J. Magn. Magn. Mater.,* 2002, **260,** p 184-187
13. K.V. Ramanujachary, M. Greenblatt, W.H. McCarroll, and J.B. Goodenough, Anomalous Electrical and Magnetic Properties of a New Quasi-Low-Dimensional Mixed-Valent Molybdenum-Cluster Compound, *Mater. Res. Bull.,* 1993, **28,** p 1257-1267